



Simulation and Estimation of Probabilities of Phases of the Pacific Decadal Oscillation

Journal:	<i>Environmetrics</i>
Manuscript ID:	draft
Wiley - Manuscript type:	Research Article
Date Submitted by the Author:	n/a
Complete List of Authors:	Nairn-Birch, Nicolas; UCLA, Statistics Diez, David; UCLA, Statistics Eslami, Esa; UCLA, Statistics Macias Fauria, Marc; University of Calgary, Biological Sciences Johnson, Edward; University of Calgary, Biological Sciences Schoenberg, Frederic; UCLA, Department of Statistics
Keywords:	PDO, sea surface temperature, simulation, time series



Simulation and Estimation of Probabilities of
Phases of the Pacific Decadal Oscillation

Nicholas Nairn-Birch¹, David Diez¹, Esa Eslami¹, Marc Macias Fauria², Edward A.
Johnson², and Frederic Paik Schoenberg¹.

¹ Department of Statistics, University of California, Los Angeles, CA 90095–1554, USA.

² Department of Biological Sciences, University of Calgary, AB, Canada.

phone: 805-215-2627
email: frederic@stat.ucla.edu or nicksbirch@stat.ucla.edu
Postal address: UCLA Dept. of Statistics
8142 Math-Science Building
Los Angeles, CA 90095–1554, USA.

Abstract

The Pacific Decadal Oscillation (PDO) index defines the leading mode of monthly sea surface temperature anomalies in the North Pacific Ocean. Time series analysis in both the frequency and time domains is applied to 107 years of monthly PDO index values. Simulations of a model fitted to the data are used to estimate p -values associated with particular events observed in the raw data. The simulations are further used to estimate the distribution of various quantities, such as the length (in years) of a positive phase, or the absolute difference between the longest positive and negative phase (in years). The results show that the probability of occurrence of a negative phase surrounded by two positive phases within a 107-year period is approximately 9.9%. The raw data's mean positive phase length is close to the simulation mean and median, while the absolute difference in maximum positive/negative phase lengths corresponds to a p -value of 14.9%. The methodology developed in this article can be useful to ecologists in assessing the potential ecological effects due to PDO variation, and for estimating the probabilities associated with future phases or other events.

1
2
3
4
5
6
7
8
9
10
11
12
13
14
15
16
17
18
19
20
21
22
23
24
25
26
27
28
29
30
31
32
33
34
35
36
37
38
39
40
41
42
43
44
45
46
47
48
49
50
51
52
53
54
55
56
57
58
59
60

1 Introduction

The Pacific Decadal Oscillation (PDO) is a large-scale scale pattern of climate variability, with a characteristic sea surface temperature arrangement in the North Pacific. It is sometimes referred to as a decade scale El Nino/Southern Oscillation (ENSO), its climatic fingerprints being most visible in the extratropics, especially the North Pacific/ North American sector [14]. The PDO has many environmental and ecological effects, from changes in regional streamflow, precipitation and temperature in North America (e.g. [15]; [16]), to marine primary and secondary productivity in the northern Pacific Ocean [24], salmon catches in eastern Asia and North America and other Pacific fish populations (e.g. [4]; [8]), and wildfires and insect outbreaks in North America ([11]; [12]; [13]). The PDO shows warm (positive) and cold (negative) phases, each of them showing different and characteristic climatic fingerprints.

Like many ecological processes, the sequences of change in the PDO often have additional compounding effects ([17]), one of them being a problem which motivated this study. The mountain mine beetle (*Dendroctonus ponderosae*, MPB) is a native beetle to Western North America [25]. A number of factors have been proposed to control MPB populations ([18]), among which larvae mortality due to cold winter temperatures and host (i.e. tree) availability are very important ones [23]. In British Columbia, Canada, winters are often too cold for the larval stages to survive [22] and host availability depends on the abundance of trees with thick phloem which provide food for their offspring to increase in numbers (i.e. trees in the ages comprised between 60 and 160 years) [1]. The occurrence of warm winter temperatures and mature pine stands (i.e. large areas of pine stands recruited approximately 110 years

before the occurrence of warm winters) would favor a MPB epidemic outbreak. This has most likely happened in the last three decades in the interior of British Columbia: where the outbreak in the 1980s caused mortality over approximately 1.84 million ha of mature pine forests, the present one (ongoing) has killed over 7.1 million ha of pine between 1999 and 2005 [2].

Winter temperatures and the age distribution of pines (and consequently their size) are controlled to a large extent by the PDO in British Columbia: while the positive phase of the PDO results in warmer winters which allow the better survival of MPB larvae [22], the negative phase of the PDO increases the frequency of persistent summer high pressure systems over the province, favoring long periods warm and dry weather that dry the forest fuel and result in large area burned [12]. In the 1890s and early 1900s the PDO was negative, and large numbers of wildfires occurred in British Columbia which produced extensive areas in the interior of British Columbia of similar age and susceptibility to MPB at the end of the 20th century. From 1976 to the present the PDO has been in a positive phase, which has resulted in milder than usual winters and high survival of MPB larvae [13]. A question motivating this study is how often can one expect such patterns of negative and positive PDO to occur.

In this paper, we develop and apply a procedure for estimating the probability of occurrence of the PDO phase regime of the last century: two positive phases separated by either a negative phase, or a *lag* or *neutral* period wherein a determinable positive/negative phase does not persist. This framework is also used to examine statistics which summarize specific phase characteristics of the PDO. The procedure consists of applying time series analysis and model fitting to existing monthly PDO time series data from the beginning of the 20th

century, and subsequent simulations of the best fitting model are examined for the occurrence of the specified phase sequence, or *event*. The probability is then estimated as the fraction of simulations in which the event occurred. By adjusting the definition of an event and singling out other patterns in the PDO, our procedure can easily be used to calculate probabilities and statistics for various regimes or characteristics of interest.

2 Data

The index created to describe the climate variation attributed to the Pacific Decadal Oscillation (the PDO index) uses monthly sea surface temperature (SST) anomalies in the North Pacific Ocean, poleward of 20 degrees north latitude. For a particular month, the index is the first principal component from an un-rotated empirical orthogonal function analysis of the difference between the observed monthly SST anomaly and the corresponding mean global average SST anomaly ([15]).

The PDO index used in this article was acquired from the Joint Institute for the Study of the Atmosphere and Ocean (JISAO) at the University of Washington; the time series data begin in January of 1900 and end in December of 2007, totaling 1284 monthly observations. A time plot of the data can be seen in Figure 1. There does not appear to be an obvious trend (systematic change in mean) in the index values, nor do the data exhibit any conspicuous seasonal fluctuation. There is a noticeable periodic fluctuation on a decadal time-scale. Positive values of the index are known to represent a positive (warm) phase, whereas negative values correspond to a negative (cool) phase.

Several studies have independently concluded that a negative phase occurred during 1900

to 1924, and again between 1947 and 1976. The PDO experienced a positive phase during 1925 to 1946, and from 1977 until the present ([9]; [14]). However, the physical mechanisms which control the PDO are not well understood; therefore, it is difficult to confidently identify a phase shift without the aid of hindsight ([14]).

3 Methods

Our approach is to fit standard time series models, such as auto-regressive moving average (ARMA) models, which may be especially well-suited to serially correlated data that is approximately stationary ([6]). Before fitting such a model, the time plot of the PDO data is examined for features of non-stationarity, as well as other distinguishing characteristics. After removing any obvious sources of non-stationarity via differencing or kernel smoothing, we proceed with the fitting of ARMA models.

One component of removal of non-stationary elements from the time series is the identification of seasonal effects or other cycles. One approach to the identification of such cycles is via spectral analysis ([19]). The spectral density function represents the contribution of different periodicities to the overall variance of a process and is an integral tool in spectral analysis. When plotted against frequency, estimates of the spectral density function form the periodogram, which helps to evince prominent frequencies responsible for the bulk of the variation in the series ([5]). For example, the periodic component, c_t , of a series can be represented as

$$c_t = \sum_r A_r \cos(2\pi w_r t + \phi_r) \quad (1)$$

where w_r are certain multiples of a fundamental frequency suggested by the periodogram,

and A_r and ϕ_r are the amplitudes and phases of the respective periodic components, which may be estimated simply by regression ([19]). Using a trigonometric identity to rearrange the parameters into linear form, (1) becomes

$$c_t = \sum_r A_r \cos(\phi_r) \cos(2\pi w_r t) - A_r \sin(\phi_r) \sin(2\pi w_r t) \quad (2)$$

In the time domain, after cyclical components and other non-stationary components (such as trend) have been removed from the time series, one may investigate the fit of autoregressive moving average (ARMA) models, which can often account for the dependence of one value on preceding observations. A standard ARMA process of order (p,q) , has the form

$$X_t = \beta_1 X_{t-1} + \cdots + \beta_p X_{t-p} + \alpha_1 Z_{t-1} + \cdots + \alpha_q Z_{t-q} + Z_t, \quad (3)$$

where $\{Z_t\}$ is a stationary white noise process. In order to determine the orders, p and q , of the process X_t , we examine the sample autocorrelation function (ACF) and sample partial autocorrelation (PACF) coefficients, and use the Akaike Information Criterion (AIC) and residual sum of squares as measures to compare and assess order combinations and their corresponding ARMA models. The final model for the PDO index results from the combination of a non-stationary periodic component and the stochastic ARMA model fitted to the stationary residuals.

Once a model that fits adequately to the PDO data has been identified, simulations can be used to inspect important practical questions, such as the statistical significance of influential trends or patterns in PDO index values. Accordingly, 1000 simulations are examined for the occurrence of the phase pattern/event defined in the Introduction. The probability associated with the phase is then estimated by the fraction of simulations in which the event occurred. The length of each simulation is constant and equal to the length

of the original data. In order to define a phase, kernel smoothing is applied to the simulated data as a low-pass filter to remove the local fluctuations that obscure the sign of a phase regime. A Gaussian kernel is used, with bandwidth h obtained using Silverman's rule-of-thumb ([7]; [20]). 95% confidence intervals are constructed for each smoothed simulation using jackknife estimates of the standard error. Values falling on either side of these bounds are then considered to be values of a (significantly) positive or negative phase regime, whereas those which do not deviate significantly from zero constitute a *lag* or *neutral phase*, wherein the identity of the PDO regime is inconclusive.

4 Results

4.1 Model fitting

Figure 1 shows a time plot of the monthly PDO index values from January 1900 through December 2007, along with a kernel smoothing of the data which allows the time interval to be divided into periods of positive, negative, and neutral phases of PDO. An initial examination does not show any systematic trend in the PDO over time; similarly, the variance appears to remain roughly constant over time. The mean PDO appears to fluctuate, but does not seem to do so in an obviously systematic manner that would indicate a severe departure from stationarity and the need to de-trend or difference the series.

Due to the noise of the monthly data, the time plot does not provide a clear indication of seasonal or periodic fluctuations. The smoothed periodogram of the raw data shown in Figure 2 reflects a large contribution from low frequencies, i.e., periods of one year or higher.

In particular, there is a noticeable spike centered around a frequency of $1/12$, as well as a region of markedly elevated amplitudes corresponding to periods of 5 and 6 years. This suggests estimating a periodic model, \hat{c}_t , with wavelengths of 12 months, 60 months, and 72 months, i.e.

$$\begin{aligned} \hat{c}_t = & -0.12361 \cos\left(\frac{2\pi t}{12}\right) + 0.1153 \sin\left(\frac{2\pi t}{12}\right) - 0.13150 \cos\left(\frac{2\pi t}{60}\right) - \\ & 0.08377 \sin\left(\frac{2\pi t}{60}\right) + 0.09978 \cos\left(\frac{2\pi t}{72}\right) - 0.05266 \sin\left(\frac{2\pi t}{72}\right) + 0.05607. \end{aligned}$$

The ACF and PACF of the residuals from the model \hat{c}_t (not shown) do not contain any obvious cutoffs indicative of a strictly moving average or autoregressive process, respectively, suggesting instead the use of an ARMA model. Table 1 contains AIC values corresponding to ARMA models of various autoregressive/moving average order combinations fitted to the stationary series. This criterion suggests that (9,7) is the best-fitting order combination, with a minimal AIC value of 2591.8. The coefficients of the ARMA(9,7) appear in Table 2.

The time plot of the standardized residuals, appearing in Figure 3, reveals several outliers exceeding three standard deviations in magnitude. However, there are no obvious patterns over time, and the model appears to adequately capture most important features of the PDO series' variation. The ACF of the residuals suggests no significant deviation from model assumptions, while the p-values for the Ljung-Box statistic are well above the threshold of significance.

The model diagnostics indicate that the ARMA(9,7) model successfully captures much of the variation in the residuals of the periodic component \hat{c}_t . Thus we henceforth consider the sum of the two series $\hat{c}_t + \text{ARMA}(9, 7)$, shown in Figure 4, as a model for the PDO. One sees from Figure 4 that the fitted model follows the PDO data closely, with noticeable deviations

only at extreme values. The residuals do not exhibit any obvious patterns over time, while their histogram and normal QQ-plot in Figure ?? are consistent with normality. Most importantly, Figure 4 shows that the model accurately captures the inter-decadal variation in positive and negative phases of the PDO index.

4.2 Simulations

One of the purposes of the present analysis is to address questions such as the probability of two significant positive PDO phases occurring before and after a significant negative PDO phase, within a period of 107 years. Examination of 1000 simulations, each consisting of 107 years of simulated, monthly PDO index values, reveals that 99 of the 1000 simulations contained such an event, namely a significant positive phases present on either side of a significant negative phase. Figure 5 shows an example of such a simulation, with the kernel-smoothed curve superimposed over the simulated data. The bandwidth determined by Silverman's rule of thumb and used in the kernel smoothing corresponds to a time span of approximately 6.75 years. It is clear that such an event (where a positive phase is followed by a negative phase, followed by another positive phase, all within 107 years) occurred in the simulation shown in Figure 5.

Since such a sequence of phases occurred in 99 out of 1000 simulations, we estimate that the probability of occurrence of this event is 9.9%, with a standard error of 0.94%. Figure 6 shows the histogram of the average length of a positive phase in the simulated PDO catalogs, as well as a histogram of the absolute differences between the longest positive and negative phases for each simulation. One sees that the observed positive phase length of 25.1 years

for the PDO data from 1900-2007 deviates only minimally from the mean of the positive phase lengths in the simulations. However, the small difference (2.75 years) in the PDO data between the length of the longest positive phase and that of the longest negative phase was somewhat unusual, corresponding to a p-value of 14.9% based on the simulations.

5 Discussion

The model developed in this article accurately reproduces the variability and defining characteristics of the PDO index since 1900. Given the current lack of knowledge of a physical mechanism of the PDO, the statistical approach presented in this study might represent a useful tool to analyze its dynamics. Of particular importance is the model's ability to capture the temporal persistence and fluctuation of positive (negative) values seen in the raw data, i.e., the low frequency variation. This characteristic has significant ecological implications both for understanding the influence of the past century's regime and predicting possible outcomes for the current century and centuries to come. Analysis of model simulations suggest that the probability of a negative phase surrounded by significantly positive phases in the next 107 years is approximately 9.9%. Accordingly, a similar large-scale fire weather regime for Western Canada in the 21st century is unlikely. The histogram for the mean length of a positive phase indicates that the apparently unusual length of time spent in a single positive phase of the PDO during the 20th century is in fact rather typical and may be anticipated to be likely to recur in the next 107 years. The absolute difference between the longest positive and negative phase of the raw data does deviate from the simulation mean. However, with a p-value of 0.149, we cannot conclude that a difference of 2.75 years

is abnormal and unexpected in a period of 107 years.

Studies show that MPB population dynamics in North America are largely dependent on the age mosaic of host trees and winter temperature mortality thresholds, which are in turn affected by PDO phase variation ([13]; [3]). As such, it is useful for ecologists to estimate the probability of a hypothetical PDO regime, or characteristic, as a proxy for assessing the likelihood of future MPB outbreaks, or other ecological events, in British Columbia and throughout North America and eastern Asia. The framework and model formulated in this article can be adjusted to investigate such probabilities. While the statistics in Figure 6 may not individually have direct ecological implications, they nonetheless demonstrate the ability to summarize and examine specific characteristics of the PDO from the model's simulations.

The statistics and probabilities determined from the simulations in this article are largely dependent on the definition of a 'phase'. The method used in this article to identify phases relies on kernel smoothed values and a jackknife confidence bound around zero to evince periods of persistently positive or negative values for each simulation. Figure ?? shows the how this method partitioned the raw data. When compared to established phase regimes reported e.g. in [9] and [14], only the first phase is defined differently by our method. This difference also raises the question of why this period, which contains predominately positive values, has occasionally been considered to constitute a negative phase, and illustrates the ambiguity in the definition of phases.

Indeed, a phase is typically defined loosely as the inter-decadal persistence of either positive or negative values, with little sign change ([14]). The phases which occurred during the 20th century were determined from visual inspection of PDO index values with the aid of hindsight and scientific consensus. As such, there is not an specific, a priori definition

which distinguishes the parameters of a ‘phase’, e.g., minimum time length, degree of sign change, etc. The absence of such parameters makes it difficult, without visual inspection, to distinguish between a positive phase and, for example, an aberrant period of positive values. This ambiguity can lead to a large range of probabilities for the same event, depending on how one parameterizes a phase. In order for accurate inference to be made from the analysis of model simulations in the future, it is important to develop a more formal and rigid definition of a ‘phase’. Our approach here, which involved using kernel-smoothing and jackknife variance estimation, is merely one suggestion.

Figure 1: Monthly PDO Index values from January 1900 to December 2007. A kernel-smoothed curve is overlaid, indicating significantly positive and negative phases, as well as neutral phases.

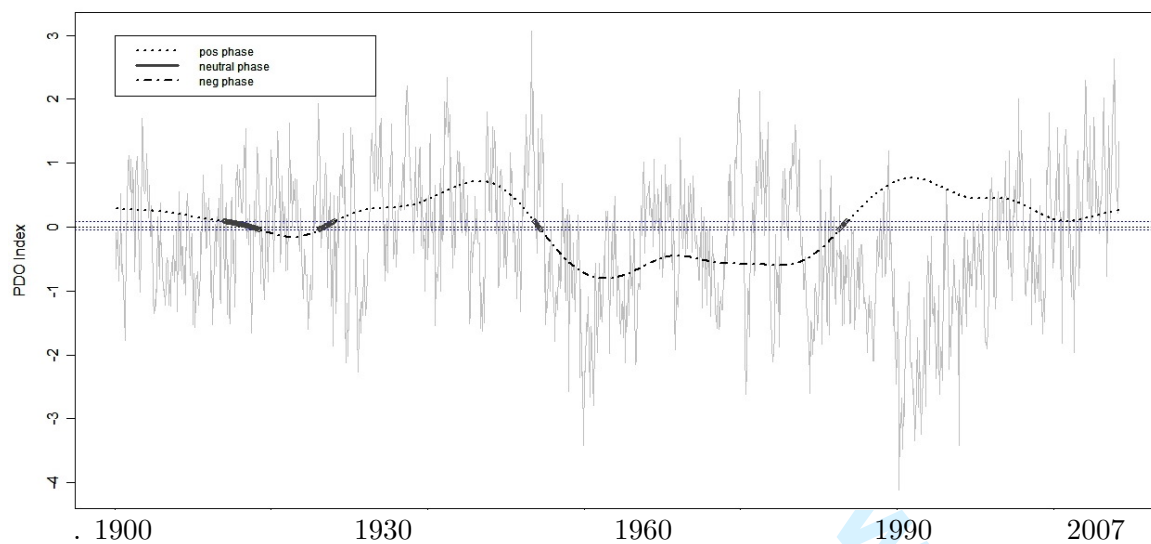


Figure 2: Smoothed periodogram of raw PDO data. Vertical lines indicate frequencies of 1/12 and 1/72, i.e. 1 cycle per 12 months and 1 cycle per 72 months, respectively. Amplitudes are in decibels.

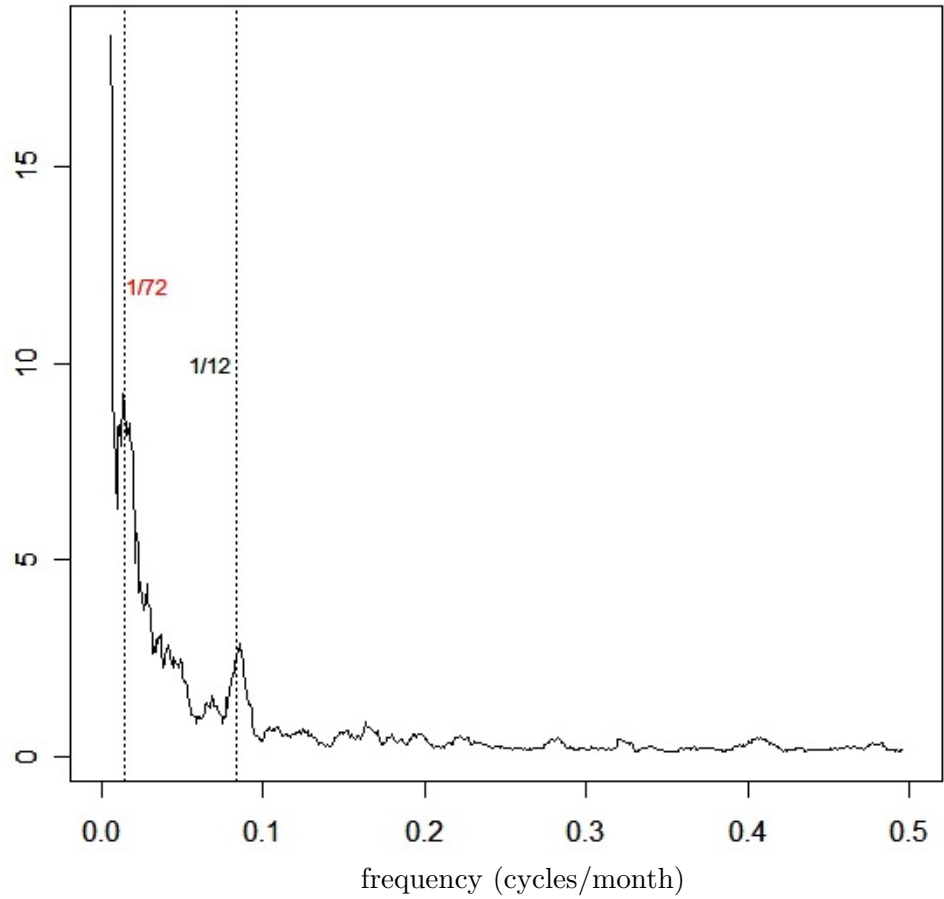


Figure 3: Time-plot, auto-correlation function, Ljung-Box p-values, and normal quantile plot for the residuals of ARMA(9,7) model. Time and lags are recorded in months.

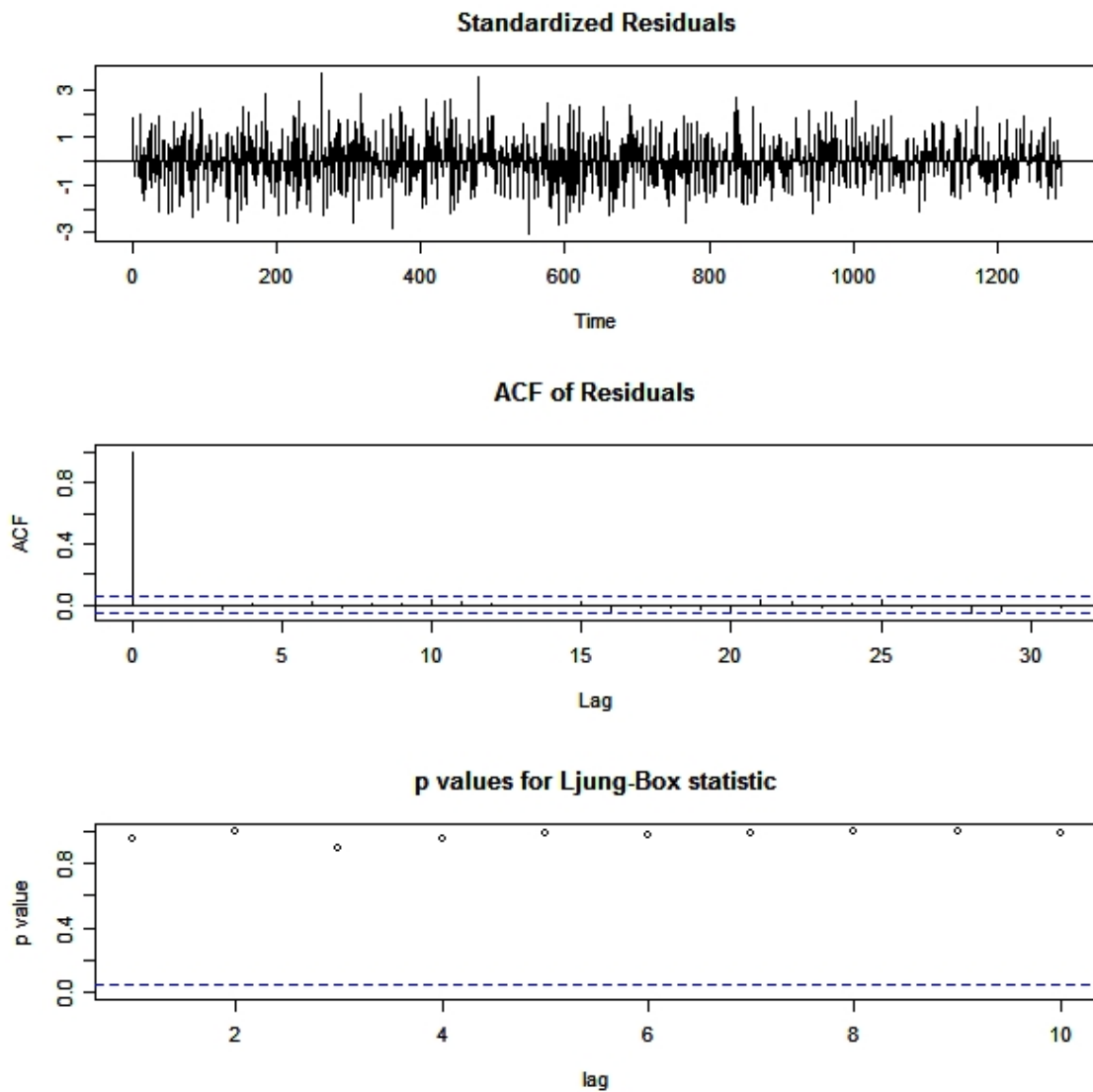


Figure 4: Time plot of the model $\hat{c}_t + \text{ARMA}(9, 7)$ and raw PDO data.

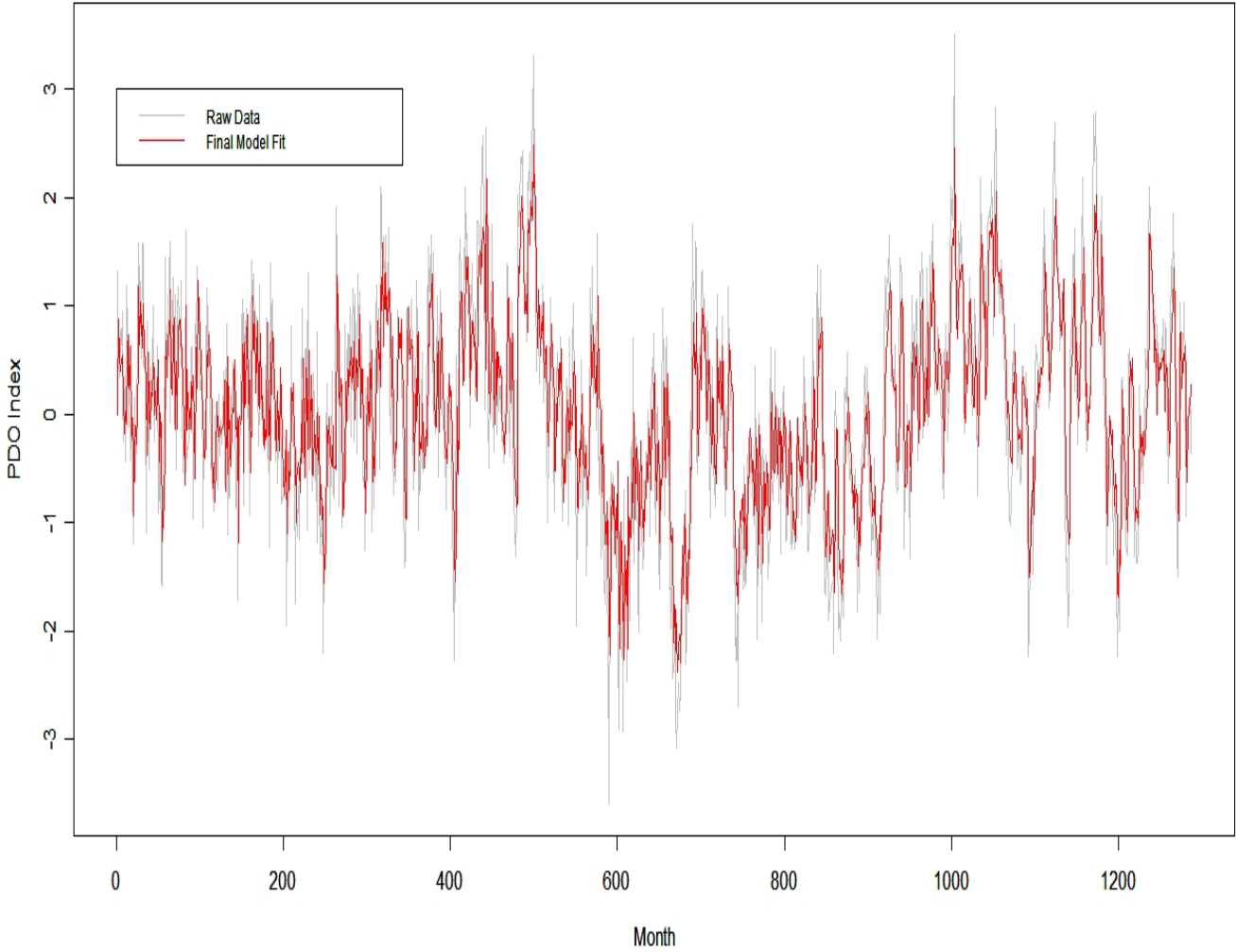


Figure 5: Sample simulation containing the occurrence of a negative phase surrounded by two positive phases.

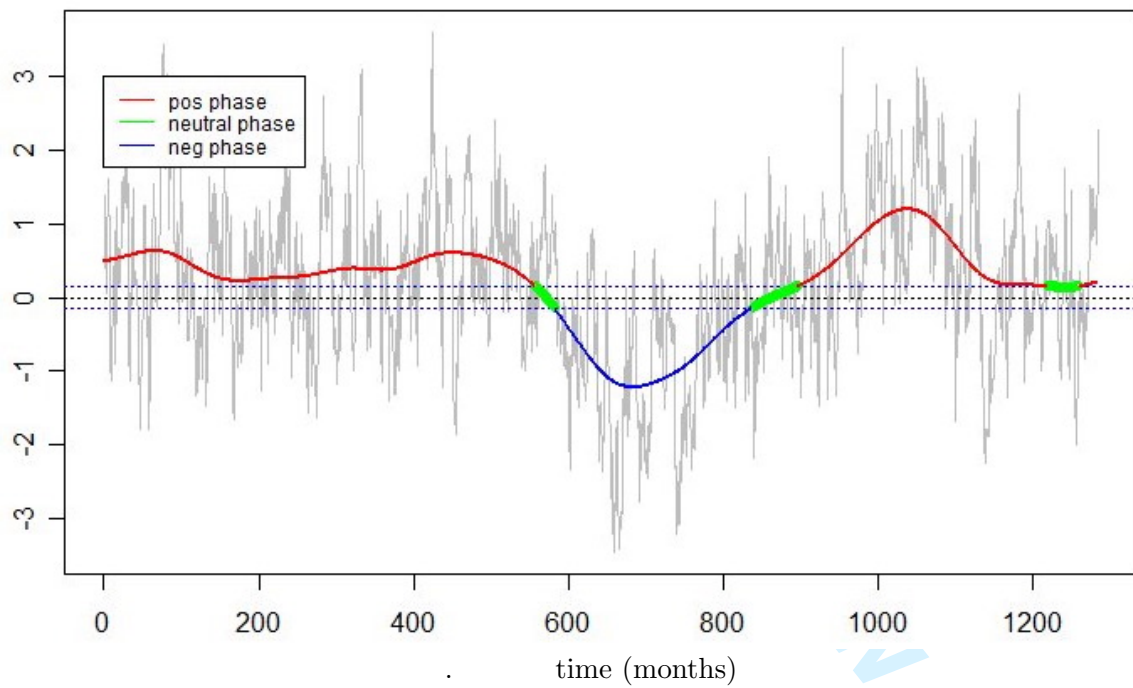
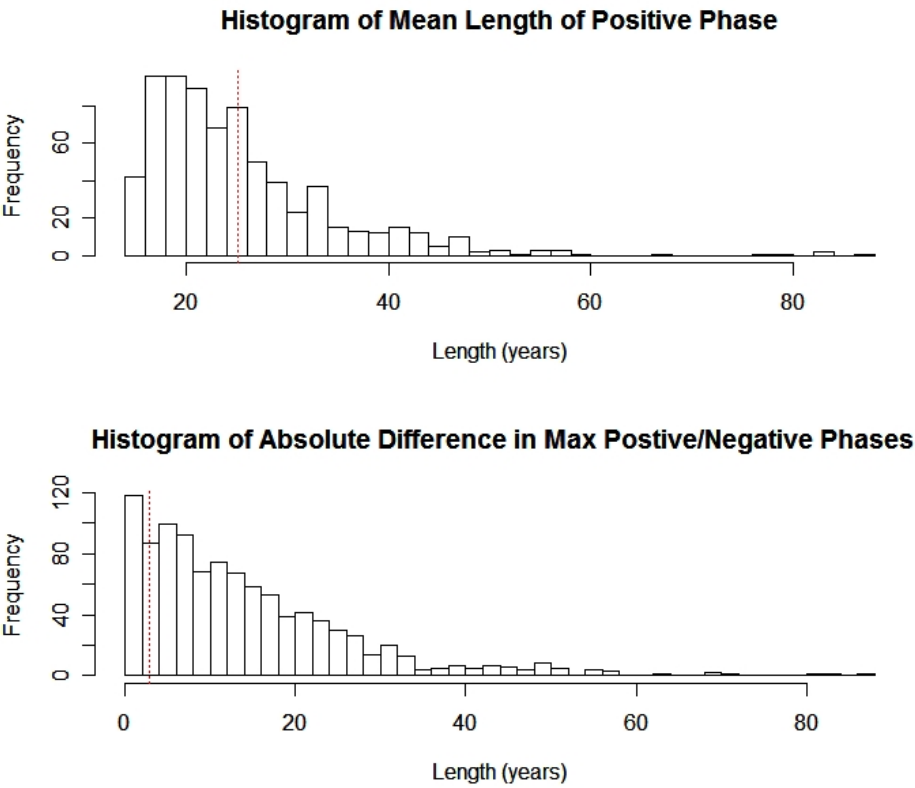


Figure 6: Histograms of mean length (years) of positive phases and absolute difference (years) in maximum positive/negative phases lengths from simulations. Dashed vertical lines indicated the corresponding values observed in the PDO data from 1900-2007.



References

- [1] Amman, G.D., Mountain pine beetle brood production in relation to thickness of lodgepole pine phloem. *J. Econ. Entomol.* 65, 138-140, 1972.
- [2] Aukema, B.H., Carroll, A.L., Zhu, J., Raffa, K.F., Sickley, T.A., and Taylor, S.W., Landscape level analysis of mountain pine beetle in British Columbia, Canada: spatiotemporal development and spatial synchrony within the present outbreak, *Ecography*, 29, 427-441, 2006.
- [3] Aukema, B.H., Carroll, A.L., Zheng, Y., Zhu, J., Raffa, K.F., Moore, R.D., Stahl, K., and Taylor, S.W., Movement of outbreak populations of mountain pine beetle: influences of spatiotemporal patterns and climate, *Ecography* 31, 348-358, 2008.
- [4] Beamish, R.J., Climate and exceptional fish production off the west coast of North America. *Can. J. Fish. Aquat. Sci.* 50, 2270-2291, 1993.
- [5] Brillinger, D., Time Series: Data Analysis and Theory, *Society for Industrial and Applied Mathematics*, Philadelphia, 2001.
- [6] Chatfield C., The Analysis of Time Series, An Introduction, Fifth Edition, *Chapman & Hall*, London, 1996.
- [7] Hardle, W., *Smoothing Techniques: With Implementation in S*. Springer, New York, 1991.
- [8] Hare, S.R., Mantua, N.J., and Francis, R.C., Inverse production regimes: Alaskan and West Coast Salmon. *Fisheries*, 24, 6-14, 1999.
- [9] Joint Institute for the Study of the Atmosphere and Ocean (JISAO) at the University of Washington, <http://jisao.washington.edu/pdo/>.

[10] Latif M., and Barnett, T.P., Causes of decadal climate variability over the North Pacific and North America, *Science*, 266, 634-637, 1994.

[11] Macias Fauria, M. and Johnson E.A., Climate and wildfires in the North American Boreal forest, *Philosophical Transactions of the Royal Society Biological Sciences*, 2007.

[12] Macias Fauria, M., and Johnson, E.A., Large-scale climatic patterns control large lightning fire occurrence in Canada and Alaska forest regions. *J. Geophys. Res.* 111, G04008, 2006.

[13] Macias Fauria, M. and Johnson, E.A., Pacific Decadal Oscillation control of mountain pine beetle outbreaks in Western Canada, *Journal of Geophysical Research*, 2008 (in review).

[14] Mantua, N.J., and Hare, S.R., The Pacific Decadal Oscillation, *Journal of Oceanography*, 58, 35-44, 2002.

[15] Mantua, N.J., Hare, S.R., Zhang, Y., Wallace, J., and Francis, R.C., A Pacific interdecadal climate oscillation with impacts on salmon production. *Bulletin of the American Meteorology Society*, 78, 1069-1079, 1997.

[16] Minobe, S., Spatio-temporal structure of the pentadecadal variability over the North Pacific. *Progress in Oceanography* 47, 381-408, 2000.

[17] Nigam, S., Barlow, M., and Berbery, E.H., Analysis links Pacific decadal variability to drought and streamflow in United States. *EOS*, Vol. 80, No. 61, 1999.

[18] Safranyik, L., and Carroll, A.L., The biology and epidemiology of the mountain pine beetle in lodgepole pine forests, in *The Mountain Pine Beetle: A Synthesis of Biology, Management, and Impacts in Lodgepole Pine*, edited by L. Safranyik, and W.R. Wilson, pp 3-66, Natural Resources Canada, Canadian Forest Service, Pacific Forestry Centre, Victoria, British Columbia, 2006.

- [19] Shumway R.H. and Stoffer D.S., *Time Series Analysis and Its Applications, with R Examples*, 2nd ed., *Springer*, New York, 2006.
- [20] Silverman, B. W., *Density Estimation*, Chapman and Hall, London, 1986.
- [21] Skinner, W.R., Shabbar, E., Flannigan, M.D. and Logan, K. Large forest fires in Canada and the relationship to global sea surface temperatures. *J. Geophys. Res.* 111, D14106, 2006.
- [22] Stahl, K., Moore, R.D., and McKendry, I.G., Climatology of winter cold spells in relation to mountain pine beetle in British Columbia, Canada, *Climate Research*, 32, 13-23, 2006.
- [23] Taylor, S.W., Carroll, A.L., Alfaro, R.I., and Safranyik, L., Forest, climate and mountain pine beetle outbreak dynamics in western Canada, in *The mountain pine beetle: A synthesis of biology, management, and impacts in lodgepole pine*, edited by L. Safranyik and W.R. Wilson, pp. 67-94, Natural Resources Canada, Canadian Forest Service, Pacific Forestry Centre, Victoria, British Columbia, 2006.
- [24] Venrick, E.L., McGowan, J. A., Cayan, D. R., and Hayward, T. L., Climate and chlorophyll a: long-term trends in the central north Pacific Ocean. *Science*, 238, 70-72, 1987.
- [25] Wood, S.L., A revision of bark beetle genus *Dendroctonus* Erichson (Coleoptera: Scolytidae). *Great Basin Naturalist* 23, 1-117, 1963.

Table 1: AIC Values for ARMA(p,q)

$q =$	1	2	3	4	5	6	7	8
$p = 1$	2615.	2614.2	2612.6	2613.5	2615.5	2615.0	2616.1	2613.4
2	2612.3	2608.5	2610.2	2614.9	2616.9	2614.5	2616.5	2615.4
3	2610.2	2610.0	2612.4	2605.2	2603.6	2605.6	2605.6	2615.3
4	2611.1	2613.5	2601.6	2601.3	2601.5	2602.4	2603.9	2613.3
5	2616.5	2615.2	2602.1	2606.2	2605.6	2619.8	2617.2	2602.6
6	2618.4	2613.1	2603.1	2617.6	2600.8	2602.7	2604.7	2621.2
7	2619.8	2613.9	2616.8	2612.1	2606.5	2605.7	2606.8	2602.6
8	2615.1	2615.7	2608.5	2606.0	2605.7	2611.2	2598.9	2591.8
9	2615.9	2615.2	2605.4	2600.7	2600.6	2614.9	2591.8	2602.2
10	2610.5	2612.5	2606.5	2604.5	2606.5	2603.2	2605.0	2606.4

Table 2: ARMA(9,7) Parameters for Periodic Residuals

parameter	estimate	SE
AR1	0.2183	0.0673
AR2	0.3301	0.0678
AR3	0.5909	0.0422
AR4	-0.768	0.049
AR5	0.1756	0.0532
AR6	0.3657	0.0518
AR7	0.7141	0.0414
AR8	-0.5666	0.0549
AR9	-0.0984	0.0409
MA1	0.3649	0.0586
MA2	0.0168	0.0722
MA3	-0.5029	0.0721
MA4	0.5157	0.0578
MA5	0.1122	0.0651
MA6	-0.2843	0.0708
MA7	-0.8549	0.0579
intercept	0.0094	0.1694